USE OF BOREHOLE-RADAR METHODS TO MONITOR THE MOVEMENT OF A SALINE TRACER IN CARBONATE ROCK AT BELVIDERE, ILLINOIS

J. W. Lane Jr., P. K. Joesten, and F. P. Haeni
U.S. Geological Survey, 11 Sherman Place U-5015, Storrs, CT 06269
jwlane@usgs.gov, pjoesten@usgs.gov, phaeni@usgs.gov

Mark Vendl, Doug Yeskis
U.S. Environmental Protection Agency, 77 West Jackson Boulevard, Chicago, IL 60604
vendl.mark@epamail.epa.gov, yeskis.douglas@epamail.epa.gov

ABSTRACT

Common-depth (CD) radar surveys and cross-hole radar tomography methods were used to monitor the movement of a saline tracer in a dual-porosity dolomite aquifer at Belvidere, Illinois. The tracer test was conducted using an array of six open-hole bedrock wells at the Parson's Casket Hardware Superfund site. The injection and recovery boreholes were about 20 m (meters) apart, and the imaging boreholes were arranged to provide planar coverage across and along the anticipated tracer path. A hydraulically conductive zone identified during previous investigations was isolated using straddle packers and pumped to establish a hydraulic gradient between the injection and recovery wells. A sodium chloride (NaCl) solution was continuously injected into this zone to move the tracer across the tomographic image plane.

CD cross-hole radar surveys and cross-hole tomography surveys were conducted before and periodically during the tracer injection. Background tomograms contain similar radar velocity and attenuation changes with depth, consistent with a layered dolomite that has variable porosity and electrical conductivity. Slow changes in attenuation associated with low tracer velocity permitted the acquisition of multiple CD surveys and two cross-hole tomography surveys during injection. CD surveys were used to rapidly identify the presence of tracer between wells. Attenuation-difference tomograms contain attenuation increases that delineate the spatial distribution with time of the saline tracer and show the progressive movement of the tracer within the tomographic image plane. Formation porosity and resistivities calculated from radar velocity and attenuation tomograms were used to estimate changes in fluid resistivity and tracer concentration in the tomographic image plane.

INTRODUCTION

Cross-hole radar tomography methods have been used in conjunction with saline tracers to interpret permeable zones and identify transport paths in fractured rock (Ramirez and Lytle, 1986; Niva and others, 1988; Olsson and others, 1992; Lane and others, 1996; Wright and others, 1996) and in unconsolidated sediments (Kong and others, 1994). Introducing a saline (electrically conductive) tracer into an aquifer such that an electromagnetic pulse propagating between the radar transmitter and receiver intersects a saline region will increase the apparent attenuation of the wave with respect to a background attenuation. Attenuation-difference tomograms that contain regions of increased attenuation identify the interwell spatial distribution of the saline tracer. Attenuation-differencing methods assume steady-state conditions so that significant electrical conductivity changes do not occur during the radar data acquisition. Steady-state methods provide a means of identifying permeable zones, but these methods do not show changes in tracer concentration or distribution with time.

The ability to monitor the movement of a saline tracer as it crosses the tomographic image plane would provide important insights and constraints on the nature of fluid flow and solute transport in an aquifer. In the absence of rapid (or multi-channel) radar systems that are able to record attenuation changes in real time, imaging tracer movement using cross-hole radar methods with currently available hardware requires a modification of the tracer injection and/or radar data acquisition procedures. Possible modifications to the experimental procedures include (1) reduction of the injection and pumping rates to

decrease the hydraulic gradient between the injection and pumped well to retard the tracer velocity to the extent that no significant changes in attenuation due to tracer movement occur during cross-hole surveying, or (2) repeated injection and pumping cycles. Repeated surveying of small sections of the aquifer during a single injection minimizes between-survey attenuation changes. Surveying different parts of the interwell region during subsequent injections to complete the entire cross-hole survey would provide kinematic radar attenuation information of the tracer traversing the image plane.

In this paper, we present the results of cross-hole radar surveys conducted in conjunction with a low-hydraulic gradient saline-tracer injection experiment in carbonate rocks at a contaminated site in Belvidere, Illinois.

FIELD EXPERIMENT

The field experiment was conducted in September 1996 at the Parson's Casket Hardware Superfund site in Belvidere, Illinois (fig. 1). Bedrock at the site consists of fractured, vuggy, argillaceous dolomite with numerous shale partings overlain by about 10 m of glacial drift. The bedrock aquifer has been characterized as a dual-porosity block and fissure system with ground-water flow occurring in vertical fractures, horizontal solution zones, and bedding-plane fractures or partings (Mills, 1993; Paillet, 1997).

An array of six open-hole bedrock wells was used for the experiment (fig. 2). The boreholes have been studied using borehole-geophysical methods and hydraulic tests (Paillet, 1997; R. T. Kay, U.S. Geological Survey, written commun., 1997). The studies identified two populations of permeable fractures, subhorizontal and subvertical, that provide hydraulic connections between several boreholes and between two horizontal, permeable, matrix-porosity zones. The permeable zones, which are located at depths of about 20 and 46 m, provide a horizontal hydraulic connection across the well field (fig. 3) (Paillet, 1997).

Boreholes T1 and T6, which are located about 20 m apart, were used for injection and pumping (fig. 2). A section of the lowermost hydraulically conductive zone in T1 and T6 between 44.2 and 47.2 m was isolated using straddle packers (fig. 3). The packed-off interval in T6 was pumped at about 11.5 L/min (liter per minute), while a tracer that consisted of a NaCl solution with a concentration of about 20 g/L (grams per liter) was continuously injected into the packed-off interval in T1 at about 0.8 L/min. Radar data were collected before and during tracer injection to determine background attenuation levels and to measure the changes in attenuation resulting from the movement of tracer through the tomographic image plane.

Cross-hole Radar CD Surveys and Tomography

Radar data were collected using the RAMAC[1] borehole radar system with 60-MHz transmitting and receiving electric-dipole antennas. Background CD and tomography surveys were conducted between six well-pairs (T2-T7, T2-T8, T3-T2, T3-T8, T7-T3, T7-T8) before injection. During tracer injection, multiple CD surveys and two complete cross-hole surveys were conducted between boreholes T2 and T8 to monitor the movement of the tracer across the T2-T8 plane. The CD surveys were used during injection to monitor the progressive movement of tracer across additional planes in the well field.

Cross-hole data were collected in saturated bedrock from 16 to 62 m below top of casing (TOC). CD cross-hole surveys were acquired by lowering the transmitter and receiver in tandem from a common starting depth in 0.5-m increments down the boreholes. In addition to the CD surveys, the complete multi-offset tomography surveys consisted of 2-m x 2-m spatial transmitter-receiver sampling coverage for each well-pair. For those well-pairs where it was anticipated that tracer would traverse the image plane, data were collected with 1-m x 1-m spatial coverage from 35 to 61 m (fig. 4).

---

[1] The use of trade names in this report is for identification purposes only and does not constitute an endorsement by the U.S. Geological Survey or the U.S. Environmental Protection Agency.

Tomography Before Tracer Injection

Velocity and attenuation tomograms collected before tracer injection between well-pairs T2-T8 and T7-T3 are shown in figures 5 and 6. The average radar velocity is about 85 m/μs (meters per microsecond), and the average attenuation is about 2.3 dB/m (decibels per meter). All background tomograms contain similar variations of velocity and attenuation with depth; this is consistent with a site-wide, uniform, horizontally stratified lithologic sequence. Based on radar propagation characteristics, bedrock at the site can be divided into three major units: (1) a high-velocity low-attenuation unit that extends from below casing to about 25 m in depth, (2) a low-velocity unit that is interlayered with high- and low-attenuation zones between 25 and 55 m, and (3) a high-velocity low-attenuation unit that extends below 55 m (fig. 7). Comparison of the velocity and attenuation anomalies with drilling logs and borehole-geophysical logs indicates that high-velocity low-attenuation zones correlate with cleaner, more competent dolomite, low-velocity low-attenuation zones correlate with zones of increased porosity within cleaner dolomite, and low-velocity high-attenuation zones correlate with increased shale and/or sulfide mineral content. The lowest velocities occur within the permeable matrix-porosity zones.

CD Surveys and Tomography During Tracer Injection

The CD surveys provided a rapid means of monitoring the progressive movement of the tracer. CD surveys between well-pairs T2-T8, T3-T8, and T2-T7 were conducted periodically during injection. The only significant increases in attenuation detected during injection occur in the T2-T8 plane (fig. 8). Four CD surveys in the T2-T8 plane conducted during tracer injection began 11, 17, 31, and 37 hours after the start of injection. Attenuation increases between 45 and 50 m begin at 11 hours and continue to increase until 37 hours of injection. The continual increase in attenuation indicates that a steady-state concentration was not achieved at the termination of injection. Small increases in attenuation are observed in the CD surveys between T3-T8 and T2-T7 conducted after 39 hours. These planes provide a limit to the maximum extent of radar-detectable tracer movement toward the pumped borehole.

Two complete multi-offset tomography surveys were conducted between T2 and T8 during the injection of tracer, from 12 to 17 hours and 33 to 37 hours after the start of the injection test. Direct-arrival amplitudes were converted to 'residual' attenuation data using the method described by Niva and others (1988). The residual attenuation of a ray is the quotient of the measured amplitude with respect to a modeled amplitude for a ray traveling through a homogeneous medium with an constant average attenuation:

$$\alpha_{residual} = -20 \log 10 \left[A_{ref} / A_{meas}\right]\left[e^{-\alpha avg\, r} \left(D(\theta_{tx})\, D(\theta_{rx})\right)\right] / r\,, \qquad (1)$$

where:

$\alpha_{residual}$ = residual attenuation (decibels)
A_{ref} = reference amplitude
A_{meas} = measured amplitude
α_{avg} = average attenuation (dB/m)
r = distance between transmitter and receiver
$D(\theta_{tx,rx})$ = directional gain function for transmitting (tx) or receiving (rx) antenna.

Effects of the saline tracer on ray attenuation were determined by subtracting the background residual attenuation from the tracer residual attenuation. After differencing, the residual-attenuation data were inverted using a conjugate gradient inversion program TOMOCG (Ivansson, 1984). A cell size of 1 m x 1 m was used for the inversion. Differences in residual attenuation should be small for tracer-free raypaths, limited by noise induced by factors such as differences in antenna battery output, errors in antenna placement, digital sampling effects, or random noise. The analysis of multiple cross-hole measurements in this study indicates that differences in the residual attenuation of a given ray less than about 0.02 dB/m are insignificant.

The attenuation-difference tomogram between background values and those existing after 12 to 17 hours of injection is shown in figure 9. A high-attenuation anomaly is observed near T2 between 44 and 48 m. The tracer appears to be spreading across the image plane towards T8.

The attenuation-difference tomogram between the background levels and those existing after 33 to 37 hours of injection is shown in figure 10. The high-attenuation anomaly present in the first difference tomogram (fig. 9) has increased in size, extending from 42 to 50 m. A horizontal attenuation zone is observed near 40.5 m in depth, moving toward T8; this is interpreted as a small horizontal zone of higher permeability.

In both difference tomograms, high-attenuation anomalies occur at depths above and below the injection depths (figs. 9 and 10). Assuming these anomalies are not tomographic reconstruction artifacts, their distribution suggests a flow pattern involving vertical (perhaps fracture controlled) transport of the tracer into the upper permeable zone and down towards the lowest radar-velocity area within the deeper permeable zone.

ESTIMATION OF POROSITY, FLUID RESISTIVITY, AND TOTAL DISSOLVED SOLIDS

Tomogram radar velocities were used to estimate porosity in the formation using a two-phase dielectric mixing formula developed by Sihvola (1989) by calibrating the relative dielectric constant of the rock matrix (e_r =8.93) to the average formation porosity of 12.84 percent (derived from laboratory analysis of 17 core samples) (Mills and others, 1997). Figure 11 shows the radar-derived porosity between T2 and T8 is shown juxtaposed to a neutron porosity log from T1 (F. L. Paillet, U.S. Geological Survey, written commun., 1997) and core-derived porosities. The radar-derived porosities match the trend in porosity observed in the neutron-log and core data. The radar-derived porosities are smoother than the neutron log and core porosities, which may reflect the horizontal averaging of the hole-to-hole radar measurements compared to the point measurements of the neutron log and core samples.

Tomogram attenuation values were used to estimate an effective resistivity according to:

$$\rho \cong 4.343\mu v/\alpha , \qquad (2)$$

where:

ρ= resistivity (Ω-m)
μ= magnetic susceptibility (H/m)
v= velocity (m/s)
α= attenuation (dB/m).

Fluid resistivities were estimated by fitting Archie's equation to the porosity and resistivity values calculated from the velocity and attenuation tomograms:

$$\rho_w = a\rho_{obs}\phi^{m}, \qquad (3)$$

where:

ρ_w = fluid resistivity
ρ_{obs}= resistivity estimated from attenuation tomogram using (2)
ϕ = porosity estimated from velocity tomogram using Sihvola (1989)
$a \cong 1.00$
$m \cong 1.39$.

The use of Archie's equation in this form to estimate fluid resistivity is a simplification that neglects considerations of lithologic changes (such as differences in shale content), effective porosity, and fluid temperature. However, assuming these effects are constant from survey to survey, differences in estimated fluid resistivity between surveys can be attributed to changes in NaCl concentration associated with movement of the tracer into the image plane.

Estimated fluid resistivity between boreholes T2 andT8 from the 12 to 17 and 33 to 37 hour cross-hole surveys is shown in figure 12. The differences in fluid resistivity between background and the 33-to-37 hour survey was converted to total dissolved solids (TDS) using the relation (Todd, 1964) (fig. 13):

$$\text{TDS (mg/L)} \approx 6{,}000/\rho_w \,. \qquad (4)$$

The changes in TDS indicate that significant transport of tracer across the image plane took place between the two complete surveys and may show that the tracer is moving toward the upper and lower high matrix-porosity zones, possibly through steeply dipping fractures.

The cross-hole radar surveys in this study provided the only information about the presence and movement of the saline tracer. Although 1,175 L of saline tracer were injected, and 84,000 L were pumped at the recovery borehole, no recovery of the tracer was ever recorded at the pumped borehole, nor was there any indication of changes in fluid resistivity or electromagnetic-induction logs collected in the array of boreholes during the experiment. These findings illustrate the benefits of using cross-hole radar methods to obtain information on aquifer properties between boreholes.

CONCLUSIONS

Common-depth radar surveys and cross-hole radar tomography surveys were used successfully to monitor the movement and distribution of a saline tracer during a low-hydraulic gradient constant-injection test in a dual-porosity aquifer in Belvidere, Illinois. Common-depth surveys were used to rapidly identify the location and progressive movement of the saline tracer between wells. Background tomograms contain velocity and attenuation anomalies consistent with a horizontally stratified dolomite sequence with variable interlayer porosity and electrical conductivity. Attenuation-difference tomograms from cross-hole surveys conducted about 20 hours apart contain attenuation increases interpreted as changes in the distribution and concentration of the tracer in the image plane. By using simplifying assumptions, radar propagation velocity and attenuation values from tomograms were used to estimate formation porosity and electrical resistivity. Porosity and electrical resistivity values fitted to Archie's equation provide estimates of fluid resistivity that were interpreted as changes in total dissolved solids within the tomography image plane. This is particularly useful where conventional borehole logs and water sampling could not identify tracer movement. The results indicate that cross-hole radar tomography surveys can be used to monitor the movement of saline tracers, can provide information useful in the interpretation of aquifer properties, and may provide data useful for flow and transport modeling.

ACKNOWLEDGMENTS

This project was funded by EPA IAG# DW14947636-01. Although this article was co-authored by employees of the U.S. Environmental Protection Agency, it has not been subjected to Agency review and does not necessarily reflect the views of the Agency.

We would like to thank Jim Ursic, Gary Cygan, Robert Kay, Pat Mills, and Steve Robinson for their assistance during the field experiment.

REFERENCES

Ivansson, S., 1984, Crosshole investigations-Tomography and its applications to crosshole seismic measurements: Stripa Project, IR-84-08, SKB, Stockholm, Sweden.

Kong, F., Westerdahl, H., By, T.L., Kitterod, N., 1994, Radar tomography for environmental geotechnology- field and simulation tests: Proceedings, GPR'94, Fifth International Conference on Ground Penetrating Radar. Kitchener, Ontario, Canada, June12-16, p. 1249-1260.

Lane, J.W., Jr., Haeni, F.P., Placzek, G., Wright, D.L., 1996, Use of borehole radar methods to detect a saline tracer in fractured crystalline bedrock at Mirror Lake, Grafton County, New Hampshire: Proceedings, GPR'96, Sixth International Conference on Ground Penetrating Radar, Sendai, Japan, September 30-October 3, 1996, p. 185-190.

Mills, P.C., 1993, Hydrogeology and water quality of the Galena-Platteville aquifer at the Parson's Casket Hardware Superfund site, Belvidere, Illinois, 1991: U.S. Geological Survey Open-File Report 93-403.

Mills, P.C., Yeskis, D.J., and Straub, T.D., 1997, Geologic, hydrologic, and water-quality data from selected boreholes and wells in and near Belvidere, Illinois, 1989-96: U.S. Geological Survey Open-File Report 97-242.

Niva, B., Olsson, O., and Blumping, P., 1988, Radar cross-hole tomography at the Grimsel Rock Laboratory with application to migration of saline tracer through fracture zones: Nationale Genossenschaft fur die lagerung radioaktiver Abfalle, NTB 88-31.

Olsson, O., Andersson, P., Carlsten, S., Falk, L., Niva, B., and Sandberg, E., 1992, Fracture characterization in crystalline rocks by borehole radar: Pilon, J., ed., Ground Penetrating Radar, Geological Survey of Canada Paper 90-4, p. 139-150.

Paillet, F., 1997, Borehole geophysics used to characterize vertical fractures and their connections to bedding plane aquifers in dolomite: Bell, R.S. ed., Symposium on the Application of Geophysics to Engineering and Environmental Problems, Reno, Nevada, March 23-26, 1997, Environmental and Engineering Geophysical Society, p. 195-203.

Ramirez, A.L., and Lytle, R.J., 1986, Investigation of fracture flow paths using alterant geophysical tomography: Journal of Rock Mechanics and Mining Sciences and Geomechanics, Vol.23, No.2, p. 165-169.

Sihvola, A. H., 1989, Self-consistency aspects of dielectric mixing theories: IEEE Transactions on Geoscience and Remote Sensing Vol. 27, No. 4, p. 403-415.

Todd, D.K., 1964, Groundwater, Handbook of Applied Hydrology: New York, McGraw Hill, Chapter 13.

Wright, D.L., Grover, T.P., Ellefsen, K.J., Lane, J.W., Jr., and Kase, P.G., 1996, Radar tomograms at Mirror Lake, New Hampshire—3D visualization and a brine tracer experiment: Bell, R.S., and Cramer, M.H. eds., Symposium on the Application of Geophysics to Engineering and Environmental Problems, Keystone, Colorado, April 28-May 2, 1996, Environmental and Engineering Geophysical Society, p. 565-575.

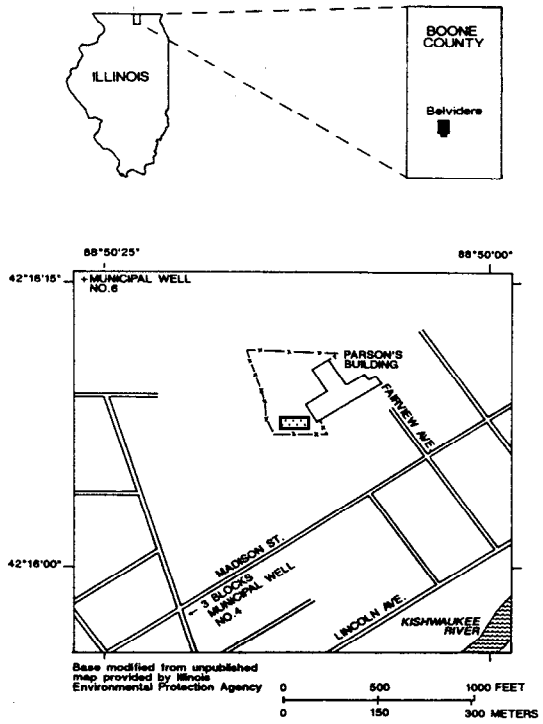

Figure 1: Location of the study area, Parson's Casket Hardware Superfund site, Belvidere, Illinois.

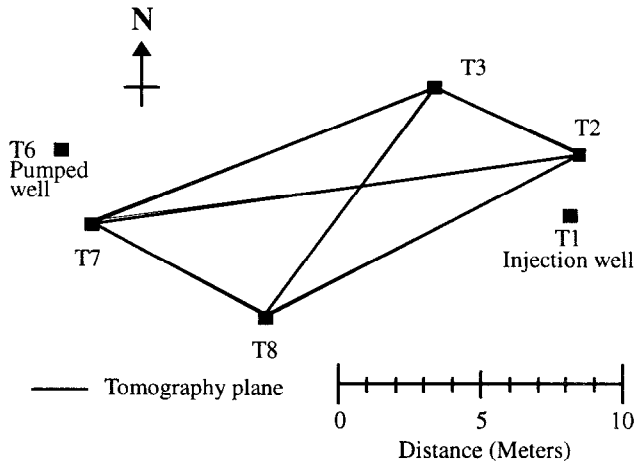

Figure 2: Borehole arrangement and alignment of cross-hole tomography planes, Parson's Casket Hardware Superfund site, Belvidere, Illinois.

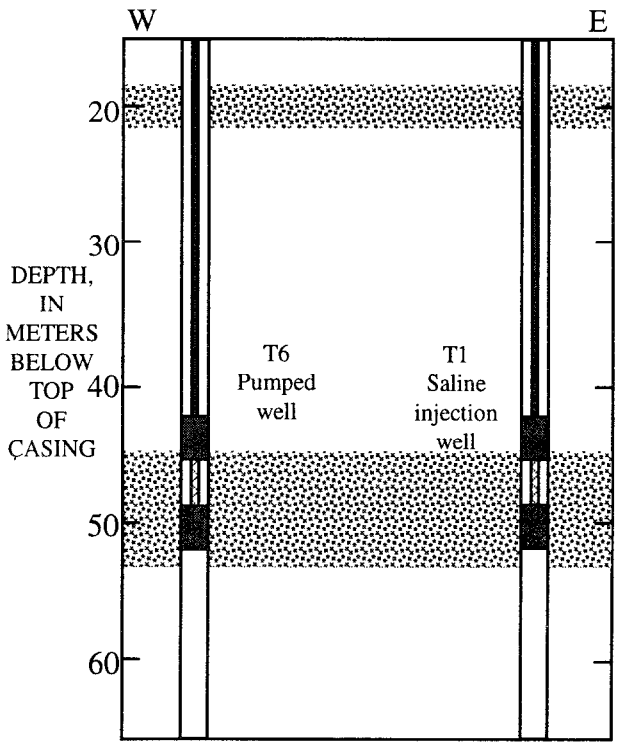

Figure 3: Location of straddle packers isolating a section of a hydraulically conductive zone that connects the pumped (T6) and injection (T1) boreholes.

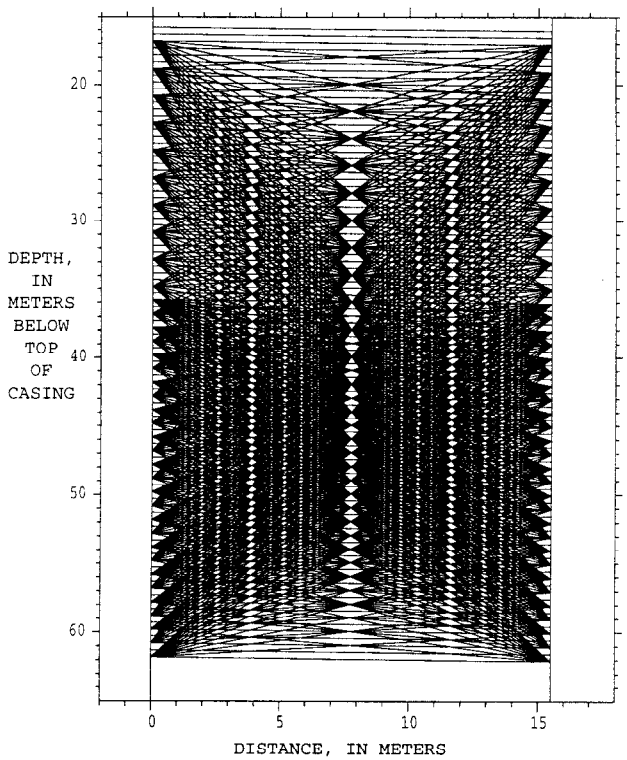

Figure 4: Cross-hole, radar-tomography transmitter-receiver geometry used in this study.

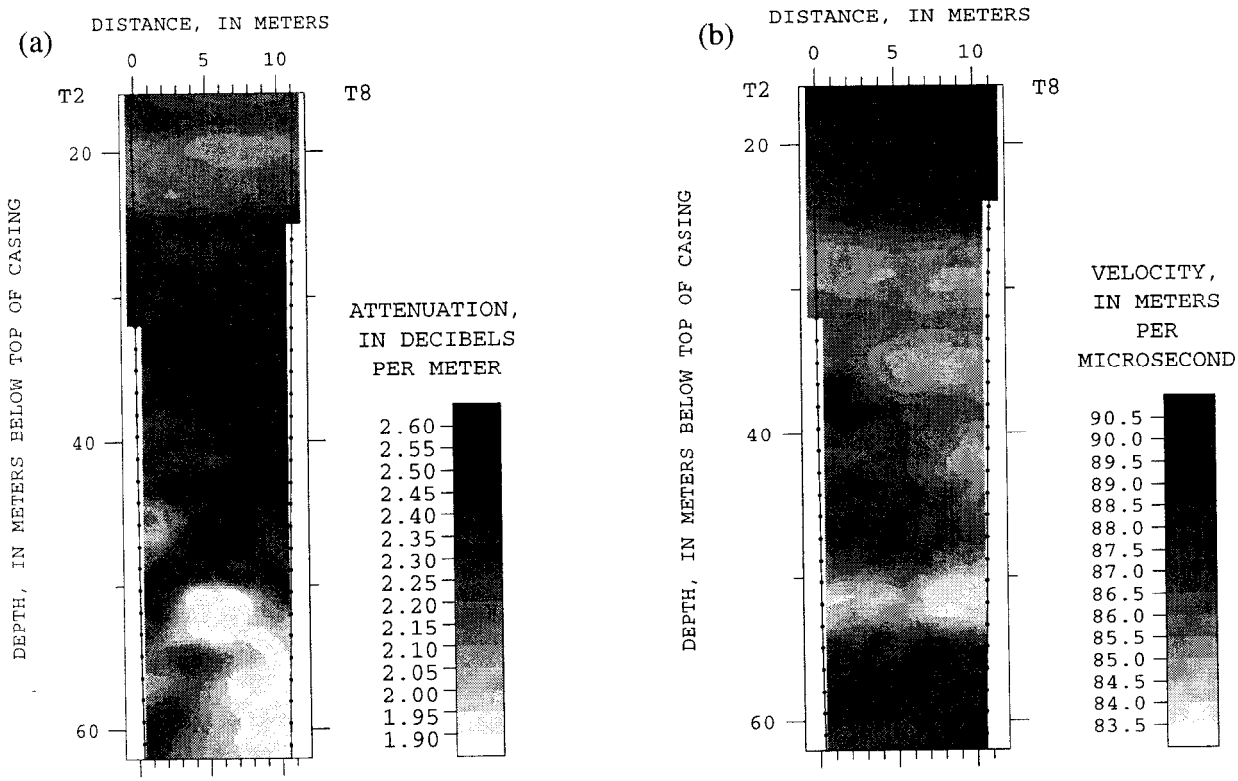

Figure 5: 60-MHz borehole-radar tomograms collected between boreholes T2 and T8: (a) attenuation tomogram (b) velocity tomogram.

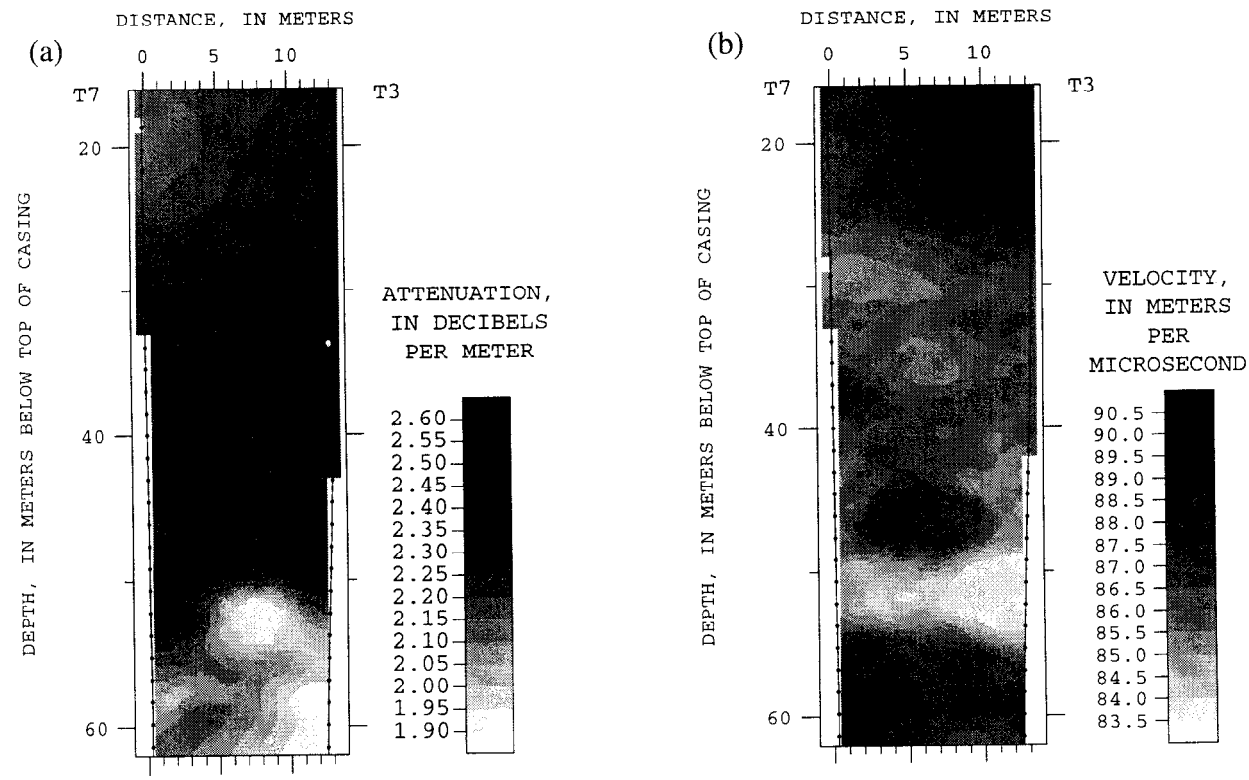

Figure 6: 60-MHz borehole-radar tomograms collected between boreholes T7 and T3: (a) attenuation tomogram (b) velocity tomogram.

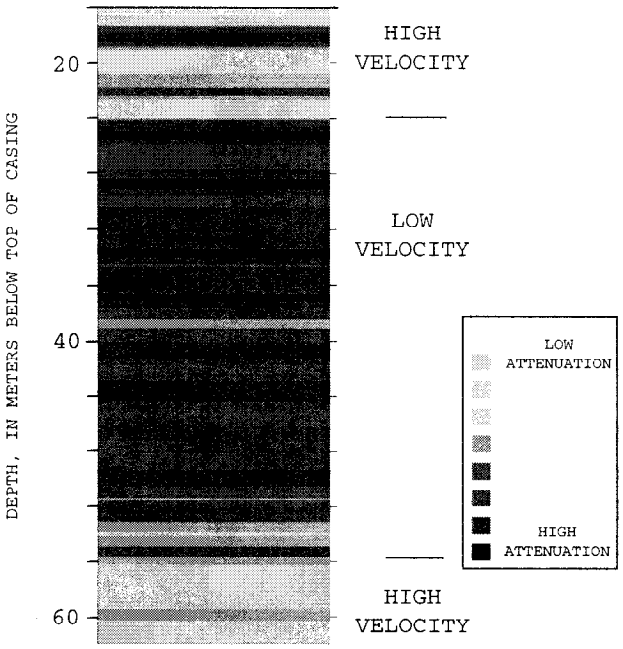

Figure 7: Conceptual model of site bedrock properties based on cross-hole radar velocity and attenuation.

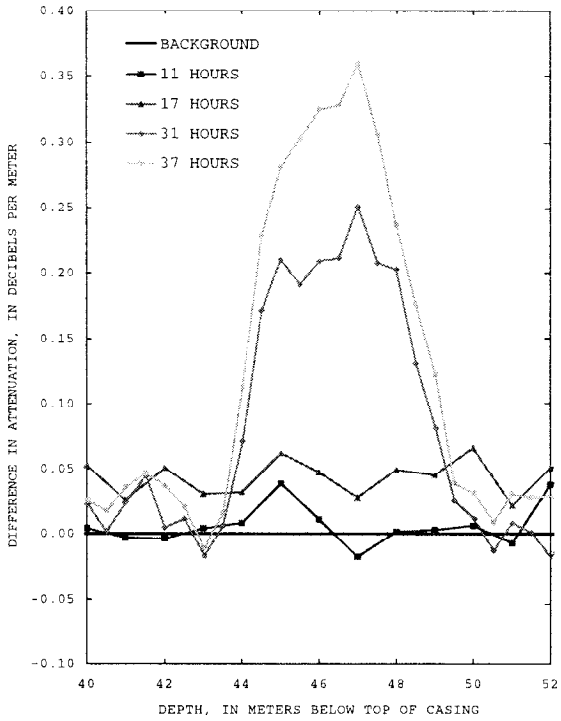

Figure 8: Cross-hole differences in attenuation between boreholes T2 and T8 from periodic common-depth surveys conducted during tracer injection.

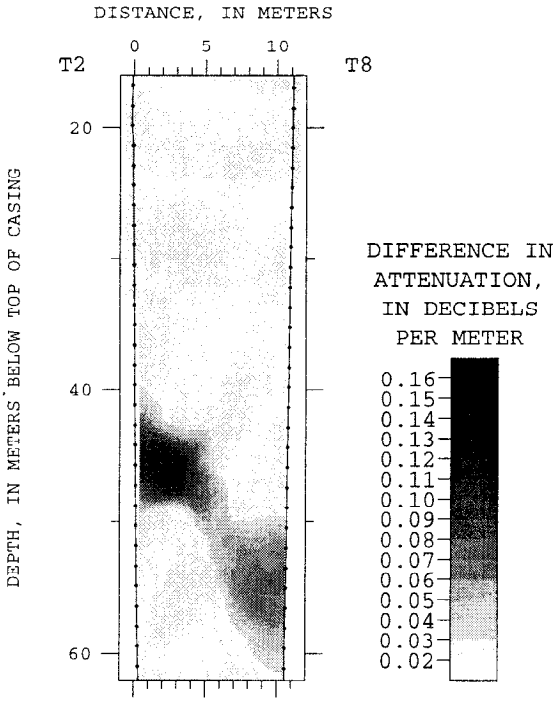

Figure 9: Attenuation-difference tomogram between boreholes T2 and T8 after 12 to 17 hours of injection.

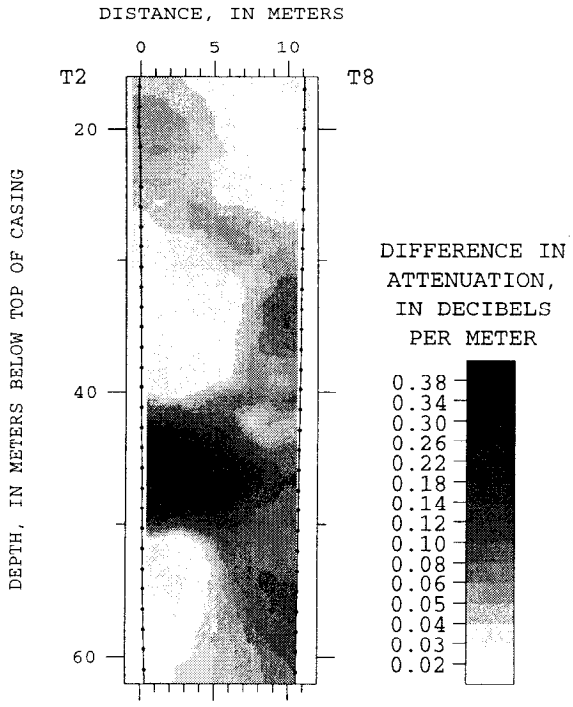

Figure 10: Attenuation-difference tomogram between boreholes T2 and T8 after 33 to 37 hours of injection.

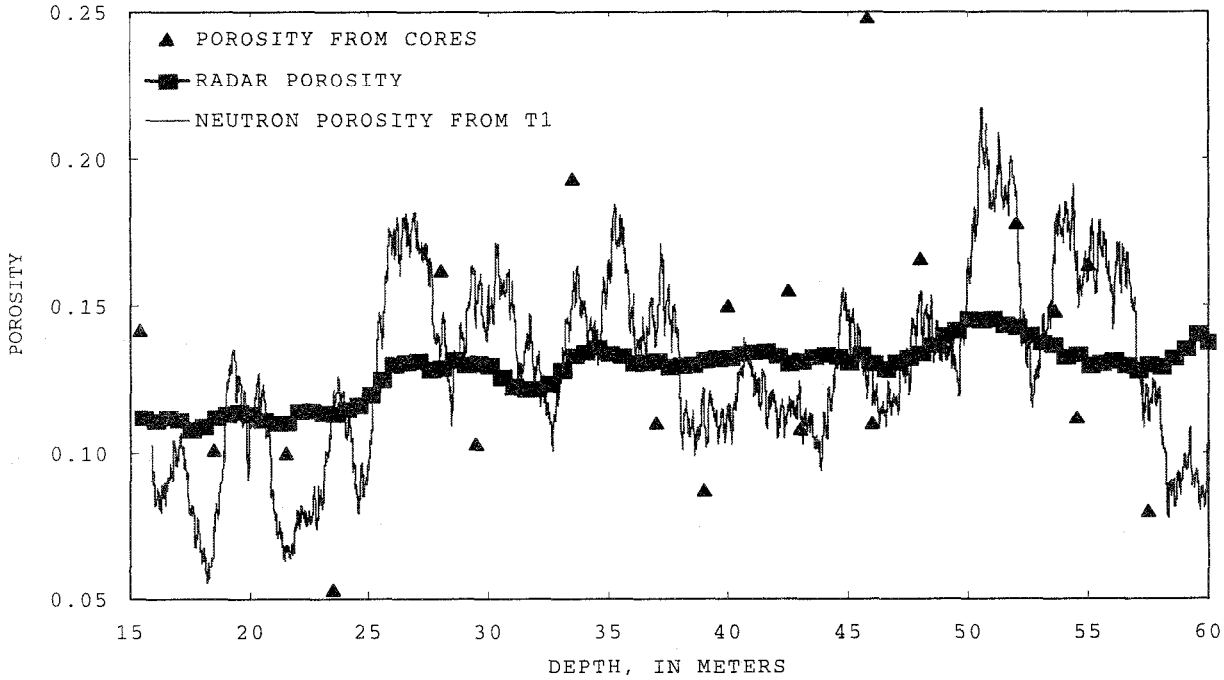

Figure 11: Porosity estimated from cross-hole radar velocity between boreholes T2 and T8 compared to porosity from rock cores and a neutron log in borehole T1.

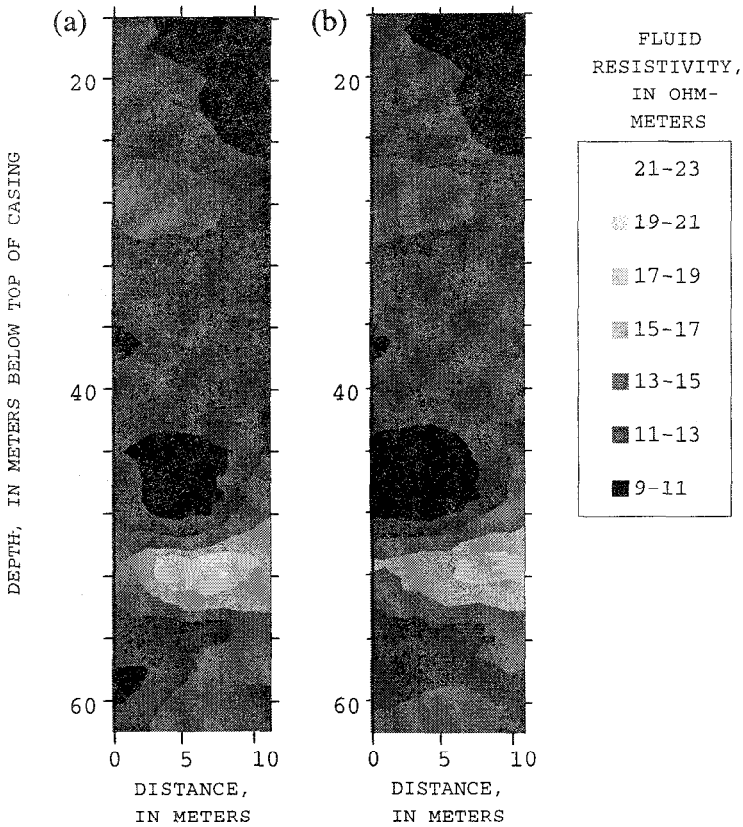

Figure 12: Estimated fluid resistivity between boreholes T2 and T8 after (a) 12 to 17 hours and (b) 33 to 37 hours of tracer injection.

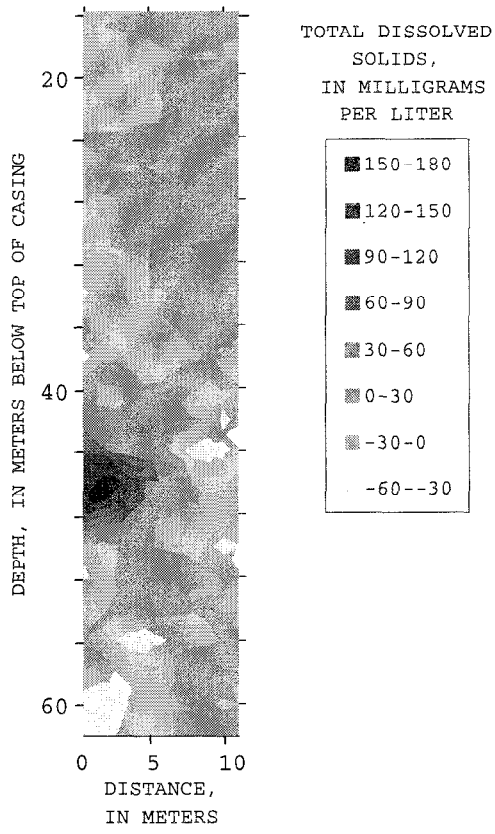

Figure 13: Estimated difference in total dissolved solids from background between boreholes T2 and T8 after 33 to 37 hours of tracer injection.